A Multi-Agent Control Based Demand Response Strategy for Multi-Zone Buildings*

Jie Cai, James E. Braun, Donghun Kim and Jianghai Hu

***Abstract*—This paper presents a multi-agent control approach for optimal demand management of multi-zone buildings. A near-optimal heuristic is proposed for a typical chilled-water air-conditioning (AC) system that can be used to formulate a demand response (DR) problem under a convex form. Then a building multi-agent control framework is utilized to synthesize a multi-agent controller where an alternating direction multiplier method (ADMM) based algorithm is adopted for intra-agent optimization and inter-agent coordination. With the proposed multi-agent DR strategy, 6% energy cost savings and 20% demand cost savings were achieved for a month period with a 3-zone case study.**

I. INTRODUCTION

Demand side management in buildings is critical for benefits of both building owners and the grid. Buildings account for more than 70% of the total electricity consumption in the US [1], so building demand behaviors play an important role in the stability and efficiency of grid operation. Utility companies provide time-of-use (TOU) pricing and a demand charge as incentives for end users to shift their load from on-peak time to off-peak time. For building owners, managing the building load in a proper way could lead to significant economic benefits.

Precooling is an effective approach to shifting building loads from on-peak to off-peak hours. With this approach, the building is slightly overcooled prior to the peak period to store 'cooling energy' in the thermal mass and during on-peak hours, the stored 'cooling energy' is released to the zone space through upward adjustments in setpoints leading to reduced cooling power. Extensive research documented in the literature has led to development of different approaches based on this idea. For example, a 25% peak cooling load reduction was demonstrated in [2] by using a precooling strategy in a large office building. With the reduced cooling load, one chiller could be eliminated that could lead to a $500,000 cost savings. In addition, monthly electricity costs could be reduced by 15%. In [3] a precooling test was carried out within an office building leading to an 80-100% chiller power reduction for a 3-hour peak period under mild weather conditions. An extended test was performed in [4] during hot summer days where the peak demand reduction only lasted for two hours and a significant rebound was observed at the 3rd hour of the peak period. To avoid the power rebound, [5] proposed a model-based demand-limiting control strategy where a data-driven model is used to predict the building thermal behavior and to maintain the cooling power at a constant level during a demand-limiting period.

Most of the aforementioned demand-limiting strategies are rule-based or rely on some simplified optimization that might lead to sub-optimal or even non-optimal solutions. In addition, the strategies only concern a single zone/building and cannot handle the demand response (DR) problem of a multi-zone building or building clusters where coordination between different end users is critical to achieve an overall optimality. In that regard, distributed model predictive control (DMPC) is a more suitable approach. There have been several attempts to apply a DMPC technique for building energy system control [6]-[8]. Most of this work has adopted a distributed control structure where each zone has a dedicated controller that optimizes its own control trajectory while different optimization and coordination algorithms were utilized in different studies. For example, a primal decomposition method was used in [6] to distribute the computation to different local controllers and a bundle method was used to solve the inter-zonal coordination. In [7], a multi-zone building control problem was formulated under a linear programming (LP) form and the Benders' decomposition method was applied.

The present study proposes a multi-agent-control-based DR strategy for multi-zone buildings where an optimizer agent is assigned to minimize energy cost of each individual zone and a demand agent is used for demand cost reduction. The main contributions and differences of the current study compared to previous work are:

1. a more detailed representation of the building heating, ventilation and air conditioning (HVAC) system is employed, so the target problem is more realistic;
2. a heuristic rule is developed for a typical chilled-water AC system that enables formulating the problem under a convex form;
3. a DR formulation is proposed that considers the tradeoff between energy cost and demand cost;
4. a distributed control scheme is proposed as a scalable alternative to address DR problems.

There is a number of benefits of adopting a multi-agent control approach in building energy systems: (1) good scalability has been demonstrated in utilizing a distributed

* Research supported by the US National Science Foundation under Grant No. 1329875.

J. Cai, J.E. Braun and D. Kim are with the School of Mechanical Engineering, Purdue University, West Lafayette, IN, USA.

J. Hu is with the School of Electrical and Computer Engineering, Purdue University, West Lafayette, IN, USA.

Email: cai40@purdue.edu

approach in the sense that the computation time increases slowly with the number of control zones (e.g., [6]); or in another sense, a centralized solution could fail for a relatively complex building control problem due to memory and computation time limitations as highlighted in [9]; (2) good reconfigurability is another advantage of employing a multi-agent controller where a component retrofit only requires local control modifications without any need to change the rest of the control system; (3) due to the distributed nature of many buildings (multi-zone, multi-story or multi-building), the multi-agent control instrumentation cost could be lower than a centralized controller when each component is equipped with an intelligent agent so that a multi-agent controller can be setup in a plug-and-play manner.

II. CASE STUDY DESCRIPTION

Three office spaces, a portion of the Living Laboratories within the Center for High Performance Buildings at Purdue University, are used as a case study building to test the effectiveness of the proposed approach. The three zones are nearly identical and the system layout is shown in Figure 1. Zone1 and Zone2 are exactly the same except for the occupancy profile, as will be shown in Section V. Zone3 differs from the other two zones in that only a single-skin facade is configured while Zone1 and Zone2 both have double-skin facades. This difference has significant effect on the building thermal behavior. In addition, Zone3 is more occupied resulting in more intensive electricity usage and internal heat gains. The three zones are served by different air handling units (AHU) but chilled-water is provided by a central air-cooled chiller as the cooling source. Hot water is provided by a boiler to the reheat coils in the AHUs. However, since the boiler efficiency is relatively constant with respect to heating demands, boiler gas usage is assumed to be proportional to the total reheat across all three zones and no boiler model is needed. There is good insulation in the separating walls so the thermal interactions between zones are negligible.

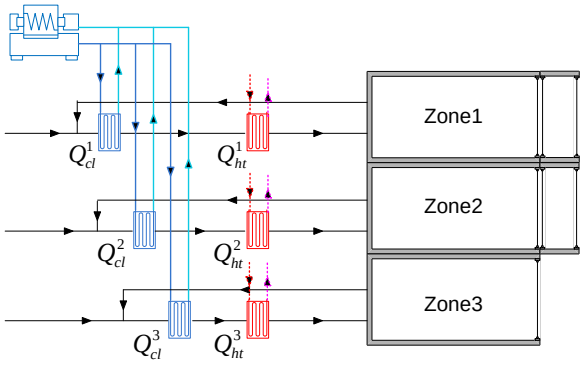

Figure 1. Case study building system layout

III. COMPONENT MODELS

Models for different components of the case study building have been constructed from field measurements except for the chiller. Extensive efforts have been made by the authors in developing efficient and robust data-driven modeling approaches for building components including envelope ([10][11][12][13]) and HVAC systems ([14]) while the present paper only focuses on the control problem. The HVAC equipment models are used in the derivation of a near-optimal heuristic rule and the envelope model is used along with the heuristic rule in the control optimization.

A. Building Envelope

A simplified thermal network model has been developed for the building envelope of each zone where the model parameters were estimated based on on-site measurements. The model details can be found in [10] or [11] and the obtained model can be formulated under a discrete-time state-space representation:

$$\mathbf{x}[i+1] = \mathbf{A}\mathbf{x}[i] + \mathbf{B}_w\mathbf{w}[i] + \mathbf{B}_u Q_z[i]$$
$$y[i] = \mathbf{C}\mathbf{x}[i] = x_z[i]$$

where $\mathbf{w}$ is a vector of uncontrollable inputs or disturbances including outdoor conditions and internal heat gains due to occupants and equipment, Q_z is the sensible cooling or heating provided to the space by the HVAC system and is the only controllable input. y or x_z is the zone air temperature.

B. Chiller

Chilled water is provided by the campus central cooling plant to the case study building. An imaginary air-cooled chiller is assumed and a data-driven model was constructed to represent the cooling plant characteristics. The model utilizes a quadratic correlation to the leaving water temperature (T_{lw}) and outdoor air temperature (T_{oa}) to calculate the chiller capacity:

$$Cap_{rate} = a_1 + a_2 T_{oa} + a_3 T_{oa}^2 + a_4 T_{lw} + a_5 T_{lw}^2 + a_6 T_{lw} T_{oa}$$

The chiller power can be calculated in exactly the same way as above, though with a different set of parameters a_1 to a_6. Under part load conditions, a quadratic correlation is used to scale down the power based on the load ratio, LR, which is defined as the ratio of the actual load to the rating capacity:

$$Pow_{PL} = \left(b_1 + b_2 LR + b_3 LR^2\right) Pow_{rate}.$$

Parameters a_1 to a_6 and b_1 to b_3 were estimated via linear regression to catalog data.

C. Cooling coil

A quasi-steady-state model was developed for the cooling coil from on-site measurements. A moving boundary modeling approach, adapted based on [15], is adopted where the transition point of the coil from dry to wet is determined iteratively with air and chilled-water energy balance. Dry and wet coil heat transfer coefficients are calculated based on correlations to air and water mass flow rates where the correlation parameters were estimated from measurements. The model details can be found in [10] and the obtained model is of the form:

$$[Q_{cl,sen}, Q_{cl,tot}] = \mathrm{ClCoil}\left(T_{ma}, RH_{ma}, T_{w,in}, m_a, m_w\right),$$

where $Q_{cl,sen}$ and $Q_{cl,tot}$ are the sensible and total capacities of the cooling coil; T_{ma} and RH_{ma} are the coil inlet air temperature and relative humidity; $T_{w,in}$ is the coil inlet water

temperature; m_a and m_w are the air and water flow rates, respectively.

D. Supply air fan and chilled-water pump

A cubic correlation to the airflow/water flow is used to calculate the supply fan/chilled-water pump power. Actual measurements were used to train the correlation parameters.

$$Pow_{pump/fan} = c_0 + c_1 m_{w/a} + c_2 m_{w/a}^2 + c_3 m_{w/a}^3$$

IV. Near-Optimal Heuristics

Integrating all the HVAC equipment models together can provide the overall HVAC system performance. Define $Q_{sen,net}$ as the cooling coil net capacity which equals the coil capacity minus the heat dissipated by the fan. This net capacity is the effective cooling rate that the AC system provides. Figure 2. and Figure 3. show the total HVAC power variations with respect to airflow under two example operating conditions. Coil inlet chilled water temperature is assumed to be a fixed value of 8.5 C. Airflow is allowed to vary between 1200 CFM (0.67 kg/s) to 2600 CFM (1.44 kg/s) for the sake of fan life span and ventilation requirement.

Figure 2. shows a case under dry coil condition. To achieve a specified net capacity (2 kW in the plotted case) higher airflow consumes more fan power and thus, requires more chiller power to compensate for the heat dissipated from the fan. This can also be observed in the coil heat exchange rate variations plotted in the bottom (the sensible and total rate curves are overlapped). Chilled water pump power is small compared to powers consumed by the chiller and supply fan. As a consequence, the total power increases monotonically with airflow.

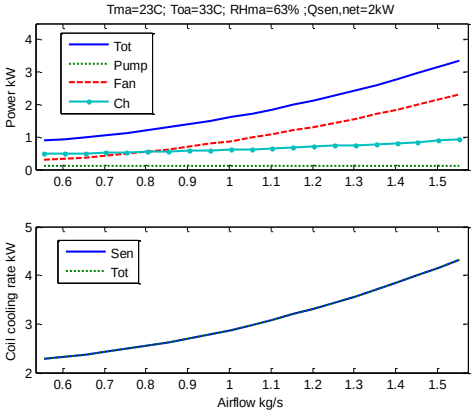

Figure 2. HVAC total power trend under dry coil condition.

Under wet coil condition shown in Figure 3. , coil sensible capacity still increases with increasing airflow to offset the fan heat. However, less dehumidification (latent capacity) occurs with higher airflow due to higher coil surface temperature and this latent capacity decrease dominates the sensible capacity increase. As a consequence, the total coil capacity and chiller power decreases with increasing airflow. A slight decrease can also be observed in the pump power because less chilled water is needed. However, the fan power increase is so dominant that the total power still increases with airflow although the curve is relatively flat when airflow falls below 1 kg/s.

A similar trend can be observed in other operating conditions, leading to a near-optimal control heuristic: maintain the airflow at minimum level and vary the chilled water flow for capacity modulation. This heuristic will be used in the DR problem formulation in the subsequent section.

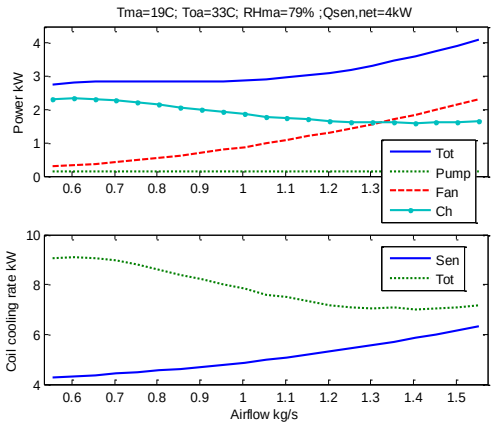

Figure 3. HVAC total power trend under wet coil condition.

V. Demand Response Problem Formulation

Equations (1) to (3) provide a formulation of the centralized DR optimization problem for the 3-zone case study described in Section II with detailed notation definitions given in the following subsection. The superscript j is used to indicate the association with zone j. By virtue of the heuristic derived in the preceding section, the coil capacity for zone j can be formulated as

$$Q_{cl,sen}^{j} = LR^{j} \cdot Cap_{rate}(\underline{T_{oa}})$$

where LR^j is the ratio of the coil load in zone j to the chiller total cooling capacity. Since coil inlet chilled water temperature is constant, the chiller capacity is only a function of the outdoor temperature T_{oa}. Note that the heuristic helps remove the total airflow (m_a) from the design variables and make the following convex formulation possible. Define Pow_{ch} as the total power consumed by the chiller and chilled water pump and a 4th order convex polynomial fit was obtained that correlates Pow_{ch} to the total load ratio LR at each outdoor air temperature:

$$Pow_{ch} = \mathrm{Pow}_{\mathrm{ch}}\left(LR, \underline{T_{oa}}\right) = \mathrm{Pow}_{\mathrm{ch}}\left(\sum_{j=1}^{3} LR^{j}, \underline{T_{oa}}\right).$$

It is shown in Appendix A that obtaining a 4th order convex polynomial fit is a convex problem and can be easily solved with a convex programming package. Figure 4. shows the variation of Pow_{ch} with respect to LR at an example outdoor air temperature T_{oa}=33C and the curve exhibits a convex shape. This convex shape can also be observed under other tested T_{oa} and because of this, good fits were obtained with R^2>0.99 for most of the tested outdoor air temperatures. Convexity of this power function makes the DR problem formulation in the following subsection convex, which provides good convergence properties for the adopted optimization algorithm. Note that the calculation of the pump power requires coil air side conditions as well as the water distribution to different zones. However, since the

pump power is small compared to the chiller power, pump power calculations are only performed under a nominal air condition and water distribution.

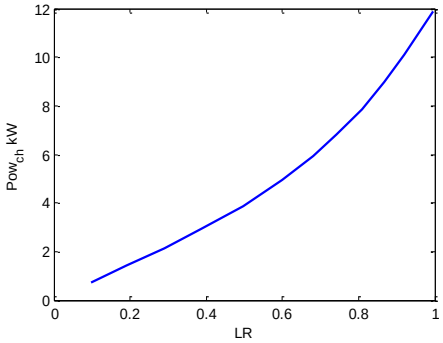

Figure 4. Variation of total power of chiller and pump with respect to load ratio.

A. *Centralized formulation*

A centralized formulation of the demand response problem is shown in (1) to (3). The cost function shown in (1) is the total utility bill increment including gas and electricity costs within the prediction period of length *Np*. r_e, $r_{DC,l}$ *and* r_{gas} are the electricity energy rate ($/kWh), electricity demand charge rate ($/kW) and gas price ($/kWh), respectively. The electricity energy rate could vary with the time of the day (e.g., on-peak and off-peak rates) so it is time indexed. Different demand charges are considered under different rating periods where P_l is the set of the time indices within period *l*. The number of demand rates or periods is denoted by *Nd*. So the formulation is flexible in handling different demand charge structures. The gas price is assumed constant (0.03 $/kWh-reheat in the case study). The first two terms of the cost function shown in (1) represent accumulated electricity energy cost and gas cost,

$$\min_{\substack{\{\mathbf{x}^j[i],LR^j[i-1],Q_{ht}^j[i-1],m_{oa}^j[i-1]\}\\ |i=k+1,\ldots,Np+k,\ j=1,2,3}} \left\{ \begin{array}{l} \sum_{i=k}^{Np+k-1}\left\{\left(\mathrm{Pow}_{\mathrm{ch}}\left(\sum_{j=1}^{3} LR^j[i], \underline{T_{oa}[i]}\right)+Pow_{nctrl}[i]\right)\cdot r_e[i]+\sum_{j=1}^{3}\left(Q_{ht}^j[i]\cdot r_{gas}\right)\right\} \\ \quad +\sum_{l=1}^{Nd}\left\{\max\left(\max_{i\in P_l}\left(Pow_{ch}[i]+Pow_{nctrl}[i]\right)-Pow_{thresh,l}[k],0\right)\cdot r_{DC,l}\right\} \end{array} \right\} \tag{1}$$

s.t.

$$Constr^j[i]:_{\substack{i=k,\ldots,Np+k-1,\\ j=1,2,3}} \left\{ \begin{array}{l} \mathbf{x}^j[i+1]=\mathbf{A}^j\mathbf{x}^j[i]+\mathbf{B}_w^j\mathbf{w}^j[i]+\mathbf{B}_u^jQ_z^j[i] \\ Q_z^j[i]=-LR^j[i]\cdot\underline{Cap_{rate}(T_{oa}[i])}+Q_{ht}^j[i]+Pow_{fan}+m_{oa}^j[i]C_{pa}\left(\underline{T_{oa}[i]}-T_{RA}\right) \\ T_{z,lb}[i+1]\le x_z^j[i+1]\le T_{z,ub}[i+1] \\ m_{oa,min}\le m_{oa}^j[i]\le m_{oa,max} \\ 0\le LR^j[i]\le 1 \\ 0\le Q_{ht}^j[i]\le Q_{ht,max} \end{array} \right. \tag{2}$$

$$\sum_{j=1}^{3} LR^j[i]\le 1,\qquad i=k,\ldots,Np+k-1 \tag{3}$$

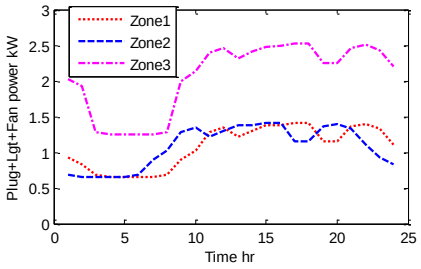

Figure 5. Non-chiller power variations for a simulation day.

Non-HVAC power needs to be considered in the DR optimization since demand is charged by the total peak power. Figure 5. shows the variation of the non-controllable power, denoted by Pow_{nctrl}, in a typical day consumed by the supply fan (supply fan power is constant providing the minimum airflow), lighting, computer and other electrical appliances. These profiles were obtained by averaging the measured power within a month. The same profile is applied to each day within the simulation test.

respectively, while the third term represents the incremental demand charge within the look-ahead horizon. $Pow_{thresh,l}[k]$ is the peak demand that occurs in rating period *l* within the past portion of the billing cycle. So the demand cost term is the incremental demand charge if the peak power within the prediction period is above the current billing cycle peak $Pow_{thresh,l}[k]$; and demand cost term is 0 otherwise. This billing cycle peak $Pow_{thresh,l}[k]$ needs to be updated after each MPC decision step if the current action leads to power consumption larger than the current $Pow_{thresh,l}[k]$.

Equation (2) lists all the optimization constraints related to each individual zone. The first constraint comes from the discrete-time dynamic model for the building envelope illustrated in Section III and Q_z is the net sensible cooling rate that the HVAC system provides. The 2nd constraint calculates the net sensible cooling rate by considering different energy sources: from cooling coil, hot-water reheat, fan heat and ventilation. Note that this constraint is originally bilinear since the return air temperature T_{RA} is the design variable T_z^j. However, this is simplified to a linear constraint by fixing the return air temperature to a constant

nominal value. This is a reasonable assumption since the zone air temperature is typically regulated within a narrow range for the sake of occupant comfort. Simulation results show that this simplification leads to less than 1% difference in the daily energy consumption. m_{oa} is the outdoor airflow rate which should be above the ventilation requirement and below the fixed total airflow. The 3rd constraint is a time varying interval type which is used to ensure thermal comfort for the occupants. The upper and lower bounds ($T_{z,lb}$ and $T_{z,ub}$) can vary depending on the occupancy status of the room. The remaining constraints in (2) are due to capacities of the specific equipment. The constraint in (3) comes from the requirement that the sum of coil cooling rates provided to different zones needs to be smaller than the chiller's cooling capacity.

B. Distributed formulation

Note that the couplings between different zones exist in both the cost function in (1) and the constraint in (3) while the constraints in (2) are already decoupled. To decouple the overall problem and to reach a distributed formulation, some new variables are introduced: $LR^j_{oth}[i]$ for j=1,2,3-- zone j's estimate of the load ratio that is consumed by the other two zones; $Pow^j_{max,l}$ for j=1,2,3-- zone j's estimate of the peak total power occurring in the rating period l within the look-ahead horizon; $Pow^4_{max,l}$-- the estimate of the peak total power for the demand agent that will be discussed shortly. In addition, define the estimate of the chiller power from zone j as

$$F^j[i] = \left(\mathrm{Pow}_{\mathrm{ch}}\left(LR^j[i] + LR^j_{oth}[i], \underline{T_{oa}[i]}\right) + Pow_{nctrl}[i]\right)/3.$$

Then the DR problem shown in (1) to (3) can be reformulated as (4) to (7).

With this reformulation, the centralized problem can be segmented into 4 sub-problems where the first 3 sub-problems concern optimal scheduling of the 3 zones and the 4th sub-problem is to minimize the demand charge.

Sub-problem j for j=1,2,3: each zone agent minimizes the electricity energy and gas cost for the corresponding zone.

$$\min_{\left\{\begin{array}{l}\mathbf{x}^j[i], LR^j[i-1], Q^j_{ht}[i-1], LR^j_{oth}[i-1], m^j_{oa}[i] \\ Pow^j_{max,l} | i=k+1,...,k+Np; l=1,...,Nd\end{array}\right\}} \sum_{i=k}^{k+Np-1}\left\{F^j[i]\cdot r_e[i] + Q^j_{ht}[i] r_{gas}\right\}$$

s.t.

$$\left\{\begin{array}{c} Constr^j[i] \\ Pow^j_{max,l} \geq \max_{i\in P_l} F^j[i]\end{array}\right\} \begin{array}{l} i = k,...,k+Np-1; \\ l = 1,...,Nd\end{array}$$

Sub-problem 4: the demand agent tries to reduce demand cost.

$$\min_{\left\{\begin{array}{l} Pow^4_{max,l} \\ | l=1,...,Nd\end{array}\right\}} \sum_{l=1}^{Nd}\left(\max\left(Pow^4_{max,l} - Pow_{thresh,l}[k], 0\right)\cdot r_{DC,l}\right).$$

Consensus constraints in (6) and (7) are required to handle the couplings across different sub-problems.

Define the global shared variable vector as

$$\mathbf{Z} := \left\{LR^j_{oth,act}[i] \,|\, j=1,2,3; i=k,...,k+Np-1\right\} \cup \left\{Pow_{max,l} \,|\, l=1,...,Nd\right\},$$

where $Pow_{max,l}$ is the actual peak demand in rating period l

$$\min_{\left\{\begin{array}{l}\mathbf{x}^j[i], LR^j[i-1], Q^j_{ht}[i-1], LR^j_{oth}[i-1], Pow^j_{max,l}, m^j_{oa}[i], \\ Pow^4_{max,l} | i=k+1,...,k+Np; j=1,2,3; l=1,...,Nd\end{array}\right\}} \sum_{i=k}^{k+Np-1}\left\{\begin{array}{r}\sum_{j=1}^{3}\left(F^j[i]\cdot r_e[i]\right) + \sum_{j=1}^{3}\left(Q^j_{ht}[i] r_{gas}\right) \\ + \sum_{l=1}^{Nd}\left(\max\left(Pow_{max,l} - Pow_{thresh,l}[k], 0\right)\cdot r_{DC,l}\right)\end{array}\right\} \quad (4)$$

s.t.

$$\left\{\begin{array}{c} Constr^j[i] \\ Pow^j_{max,l} \geq \max_{i\in P_l} F^j[i]\end{array}\right\} \begin{array}{l} i = k,...,k+Np-1; \\ j = 1,2,3; \quad l = 1,...,Nd\end{array} \quad (5)$$

$$LR^j_{oth}[i] = \sum_{s\neq j} LR^s[i], \quad i = k,...,k+Np-1; \; j = 1,2,3 \quad (6)$$

$$Pow_{max,l} = Pow^j_{max,l}, \quad j = 1,2,3,4; \quad l = 1,...,Nd \quad (7)$$

Note that the variable LR^j_{oth} is an estimate that is made from zone j, thus it belongs to zone j. The introduction of this variable helps to decouple the first term in the centralized cost function in (1) and is also used to bridge different sub-problems. The constraint in (6) illustrates the relationship of this new variable to other existing variables.

The variable $Pow^j_{max,l}$ also belongs to zone j. As a result, the constraints in (5) are separate for different zones, which are indexed by j. The introduction of $Pow^4_{max,l}$ helps separate the demand cost from the zones so that an individual agent can be assigned to handle the demand cost as will be described in the following.

and $LR^j_{oth,act}$ is the actual sum of load ratios from zones other than zone j.

For sub-problem j with j=1,2,3, the local shared variable vector is defined as

$$\mathbf{X}^j := \left\{LR^j[i], LR^j_{oth}[i] \,|\, i=k,...,k+Np-1\right\} \cup \left\{Pow^j_{max,l} \,|\, l=1,...,Nd\right\}.$$

For the demand sub-problem, the local shared variable vector is

$$\mathbf{X}^4 := \left\{ Pow^4_{max,l} \mid l = 1,..., Nd \right\}.$$

The consensus constraints in (6) and (7) are linear and thus, can be reformulated as

$$\mathbf{X}^j = \mathbf{E}^j \mathbf{Z} \qquad \text{for } j = 1,..., 4 \tag{8}$$

C. Solution scheme

A multi-agent control framework has been developed to facilitate the multi-agent control design process [10][16]. With the help of this framework, the distributed formulation can be easily composed and an alternating direction multiplier method (ADMM) based algorithm is implemented within the framework as a mechanism for intra-agent optimization (energy cost minimization within each zone agent and demand reduction in the demand agent) and inter-agent coordination (enforcing consensus constraints). The algorithm is implemented in a two-level hierarchy: local- or sub- problems are solved in parallel by the corresponding agents with the convex programming package CVX [17] and the SDPT3 solver [18]. A coordination level performs a simple multiplier variable update.

VI. Case Study Results

The case study considers typical summer electricity tariffs shown in TABLE I. which has three rating periods: on-peak, mid-peak and off-peak periods. Electricity energy cost differs slightly in different periods and only an anytime peak demand charge is involved. So there is only one demand rating period and Nd=1 in the formulation shown in (1). A 24-hr look-ahead horizon is implemented so Np=24 and only the first step decision is applied. After one time step period is past, the optimization is repeated so this procedure is carried out in a receding horizon scheme. Zone temperature lower/upper bound $T_{z,lb}$/$T_{z,ub}$ is set to 20.5/24.5C during unoccupied periods and 21.5/23.5C during occupied periods. The occupied period starts from 9am and ends at 9pm every day and the rest of the time is unoccupied. The minimum outdoor air intake is $m_{oa,min}$ =250 CFM (0.14 kg/s) for ventilation and the maximum is $m_{oa,max}$ =1200 CFM (0.67 kg/s) which is the fixed total airflow. Actual weather measurements from June 2015 were used as external excitations in the simulation test and perfect weather prediction was assumed in the MPC optimization.

Figure 6. shows the coordination iterations at an example time step. The top plot shows the consensus constraint violation, which is the L_2 norm of the mismatch between the two sides of the equality shown in (8). The bottom plot shows the variation of the total utility cost. The iterations converge to a consensus optimum in an oscillatory manner. This type of convergence was observed for all simulated steps by virtue of convexity in the proposed formulation. In addition, strict convexity provides guaranteed convergence to the global optimum which has been confirmed by comparison of the distributed and centralized solutions in the case study results. Note that the case study is relatively simple and is mainly used to demonstrate the effectiveness of the proposed approach. The size of the case study problem makes it difficult to demonstrate any computational benefits whereas a similar but larger scale case study considered in [9] has shown great computational benefits in utilizing a multi-agent controller.

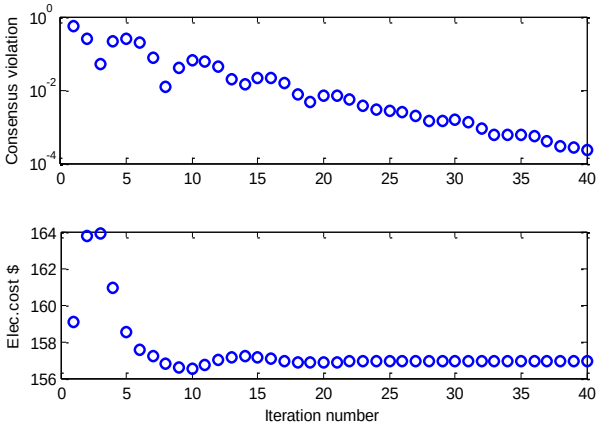

Figure 6. Convergence of solution algorithm.

To assess the cost savings potential, a baseline control was simulated where cooling is turned on when zone temperature would rise above $T_{z,ub}$ and reheat is enabled when the temperature would drop below $T_{z,lb}$. The baseline control results are shown in Figure 7. Most of the time, cooling is required to prevent the zone temperatures going beyond the comfort upper bound. The peak power consumptions occur within the period of 350 to 410 hr. A demand cost of 197$ was determined for this simulation period. TABLE II. lists the energy and demand costs associated with different control strategies.

A multi-agent DR strategy without economizer mode, which set $m_{oa,max}$=$m_{oa,min}$, was tested and the results are plotted in Figure 8. At the beginning of the simulated billing cycle, the peak demand variable $Pow_{thresh,1}$[1] is set to 0. As a result, significant precooling is observed during the first several days to limit the peak power as much as possible. This is not optimal in the scope of the whole month, since the first several days do not contain the peak load and the strategy is over-prioritizing the demand cost reduction which could lead to more energy cost. This unfair weighting continues until reaching the actual monthly peak. Because of this, there might be small or even negative energy cost savings during the period prior to the monthly peak. A remedy would be to set the starting peak demand variable $Pow_{thresh,1}$[1] to a rough estimate of the target peak. However, it was shown in [9] that the monthly cost savings would be negligible even if $Pow_{thresh,1}$[1] is set to the actual optimal value because the energy savings potential is much smaller than that for the demand. Besides the first several days, significant precooling is also present prior to the monthly peak days. The zoom-in plot in Figure 9. shows the temperatures along with the power splits for different zones within the peak load period. Zone3 has higher load than the other two zones due to the high internal gains and strong coupling to the ambient, so Zone3 has the earliest precooling start time. In addition, different zones shift their "precooling peaks" to different periods so that the total power is maintained flat. This demonstrates the benefits of inter-zonal coordination, because without coordination the zones would

possibly precool at the same time leading to another power peak.

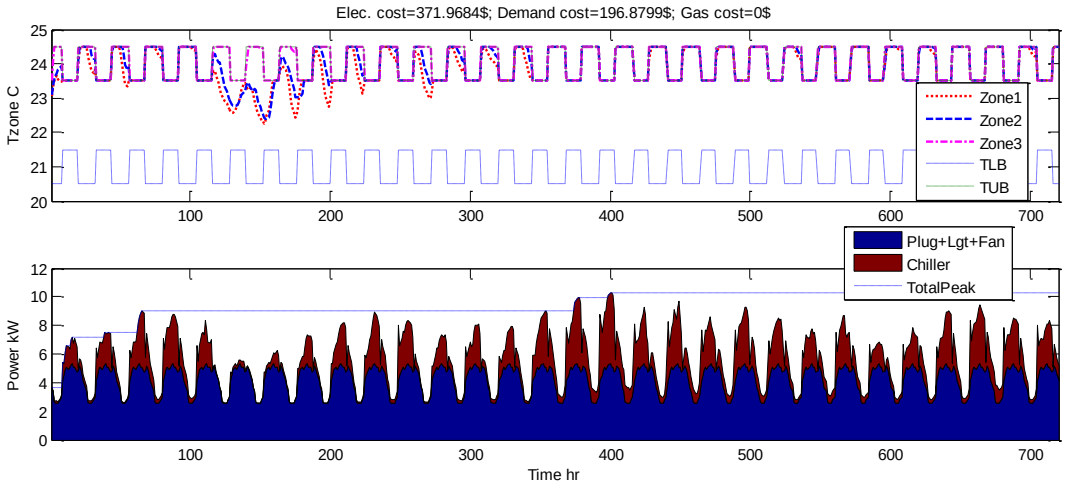

Figure 7. Simulation results under baseline control.

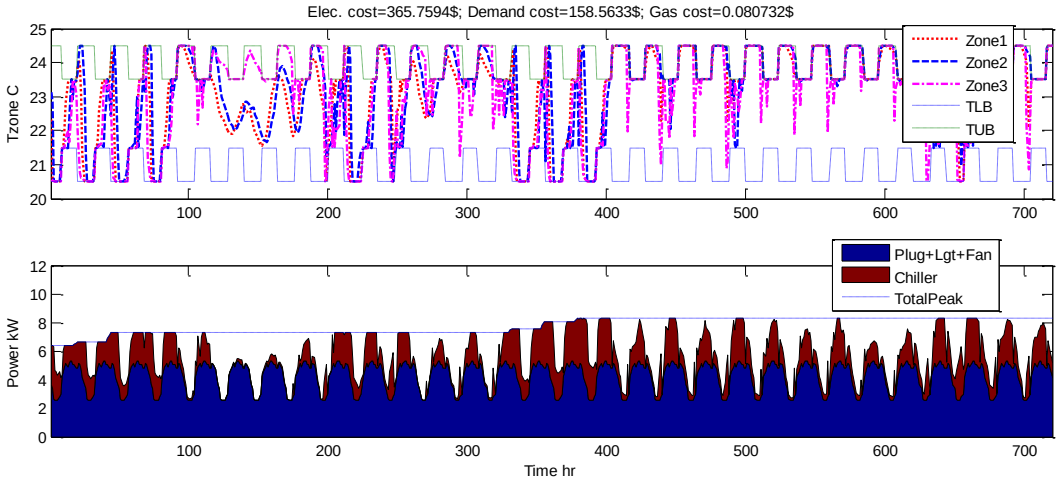

Figure 8. Simulation results under multi-agent demand response control.

This DR strategy without economizer and with $Pow_{thresh,1}[1]=0$ leads to 1.6% energy cost savings but nearly 20% demand cost savings. 5~15% savings were reported for the chiller energy cost in previous demand-limiting studies, which is comparable to the savings achieved in the present study since only 23% of the energy consumption comes from the chiller.

TABLE I. SUMMER TOU TARIFFS WITH DEMAND CHARGE

Rate periods	Electricity price ($/kWh)	Hours	Demand charge
On-peak	0.108	Noon - 6 PM	$19.2/kW anytime peak demand
Mid-peak	0.089	8 AM - noon; 6 PM - 11 PM	
Off-peak	0.064	All other hours	

Another tested strategy is the multi-agent DR with economizer where the outdoor airflow is allowed to vary within the feasible range. This strategy could take advantage of the "free cooling": intake more outdoor air when it is cool outside but space cooling is still needed. This strategy leads to significantly larger energy cost savings and also helps reduce the demand cost compared to the DR strategy without economizer mode.

TABLE II. ELECTRICITY COSTS UNDER DIFFERENT STRATEGIES

Control strategy	Electricity cost ($)		
	Energy cost	*Demand cost*	*Total cost*
Baseline	372	197	569
Multi-agent DR	366(1.6%↘)	159(19.3%↘)	525(7.7%↘)
Multi-agent DR with economizer	351(5.7%↘)	155(21.3%↘)	506(11.1%↘)

VII. CONCLUSION & DISCUSSIONS

This paper proposed a multi-agent control approach and demonstrated its effectiveness in solving the demand response problem in a multi-zone building. A key element is the integration of a near-optimal heuristic rule within the multi-agent control formulation that helps guarantee convergence of the proposed algorithm. Simulation results for a case study show that the proposed approach can provide significant demand cost reduction but energy cost savings is small without economizer operation. When an economizer is enabled, a noticeable energy cost savings is obtained by utilizing the "free cooling" and demand cost reduction is also enhanced slightly.

The proposed approach can also be applied to a building cluster with an aggregated utility bill. Different buildings could have a shared cooling source such as buildings on a campus where chilled water is provided by a central cooling plant and distributed to multiple buildings. The case study considered in this paper is representative of these opportunities since different zones could represent different buildings that are thermally decoupled from each other. For the case where each building has its own dedicated cooling system, e.g., an apartment complex, coordination is still needed among different buildings as long as an aggregated bill is used.

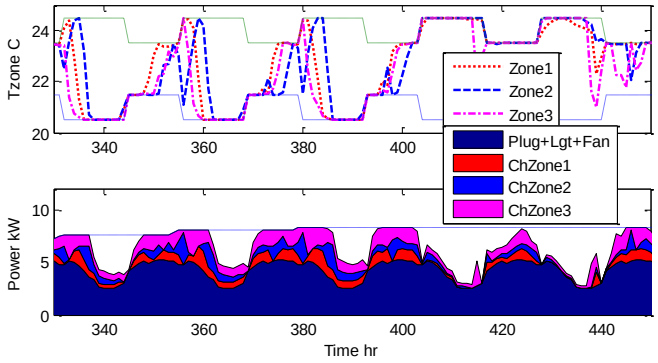

Figure 9. Zoomed plots of the peak period under DR control.

A limitation of the approach is that the HVAC model would underestimate the cooling power when dehumidification occurs. So the cost savings might be compromised under humid weather conditions and the proposed approach should be improved to better address this issue as a future work.

APPENDIX A

Given a sample of a single independent variable **x** and the corresponding observation vector **y**:

$$\mathbf{x} = \left[x_1, ..., x_N\right]^T \in \mathbb{R}^N, \quad \mathbf{y} = \left[y_1, ..., y_N\right]^T \in \mathbb{R}^N$$

and define

$$f(x \mid \mathbf{a} = [a_0, a_1, a_2, a_3, a_4]) = a_0 + a_1 x + a_2 x^2 + a_3 x^3 + a_4 x^4,$$

$$\mathbf{X} = \begin{bmatrix} 1 & x_1 & x_1^2 & \cdots & x_1^4 \\ 1 & x_2 & x_2^2 & \cdots & x_2^4 \\ \vdots & \vdots & \vdots & \ddots & \vdots \\ 1 & x_N & x_N^2 & \cdots & x_N^4 \end{bmatrix},$$

then the 4th order convex polynomial fit problem is:

$$\min_{\mathbf{a}} \left\|\mathbf{y} - \mathbf{X}\mathbf{a}\right\|_2^2$$

$$\text{s.t.} \quad \mathbf{a} \in \mathbf{A} = \left[\mathbf{a} \in \mathbb{R}^5 \mid f(x \mid \mathbf{a}) \text{ is globally convex in } x\right]$$

$$\Leftrightarrow \mathbf{a} \in \mathbf{A} = \bigcap\nolimits_x \left[\mathbf{a} \in \mathbb{R}^5 \mid f''(x \mid \mathbf{a}) \geq 0\right]$$

Note that $f''(x|\mathbf{a})$ is linear in **a** for a given x. Thus, **A** is convex since it is an intersection of an infinite number of half spaces. In addition, $f''(x|\mathbf{a})$ is quadratic in x and **A** is non-empty. So the 4th order convex polynomial fit problem is convex.

REFERENCES

[1] US EPA, Buildings and their impact on the environment: a statistical summary, 2009. http://www.epa.gov/greenbuilding/pubs/gbstats.pdf.

[2] Keeney, Kevin R., and James E. Braun. Application of building precooling to reduce peak cooling requirements. *ASHRAE transactions*, 103.1 (1997): 463-469.

[3] Xu, Peng, et al. Peak demand reduction from pre-cooling with zone temperature reset in an office building. Lawrence Berkeley National Laboratory, 2004.

[4] Xu, Peng, and Philip Haves. Case study of demand shifting with thermal mass in two large commercial buildings. *ASHRAE Transactions*, 112.1, 2006, 572.

[5] Lee, Kyoung-ho, and James E. Braun. Model-based demand-limiting control of building thermal mass. *Building and Environment.* 43.10 (2008): 1633-1646.

[6] Lamoudi, M. Y., Alamir, M. and Beguery, P., Distributed constrained Model Predictive Control based on bundle method for building energy management, *50th IEEE Conference on Decision and Control and European Control Conference*, 2011

[7] Morosan, P., Bourdais, R., Dumur, D. and Buisson J., Distributed model predictive control based on Benders' decomposition applied to multisource multizone building temperature regulation, *49th IEEE Conference on Decision and Control*, 2010

[8] Ma, Yudong, Garrett Anderson, and Francesco Borrelli. A distributed predictive control approach to building temperature regulation. *American Control Conference (ACC), 2011*. IEEE, 2011.

[9] Cai, J., Braun, J.E., Kim, D. and Hu, J., General approaches for determining the savings potential of optimal control for cooling in commercial buildings having both energy and demand charges, *Science and Technology for the Built Environment*, 2016, submitted

[10] Cai, Jie, A low-cost multi-agent control approach for building energy system management, Ph.D. dissertation, School of Mechanical Engineering, Purdue University, 2015, in preparation.

[11] Cai, Jie and Braun, James E., A practical and scalable inverse modeling approach for multi-zone buildings, 9*th International Conference on System Simulation in Buildings, Liege, Belgium, 2014*

[12] Cai, Jie and Braun, James E., An inverse hygrothermal model for multi-zone buildings, *Journal of Building Performance Simulation*, 2015

[13] Cai, Jie, Kim, Donghun, Braun, James E. and Hu, Jianghai, Optimizing zone temperature setpoint excitation to minimize training data for data-driven dynamic building models, *American Control Conference*, 2016, to appear.

[14] Cai, Jie and Braun, James E., Gray-box modeling of multi-stage direct-expansion (DX) units to enable control system optimization, *ASHRAE Transactions*, 2015

[15] Braun, James E., Methodologies for the design and control of central cooling plants, Ph.D. dissertation, University of Wisconsin, Madison, 1988.

[16] Cai, J., Kim, D., Jaramillo, R., Braun, J.E. and Hu, J., A general multi-agent control approach for building energy system optimization, *Energy and Buildings*, 2015, accepted with minor revision

[17] Grant, Michael, Stephen Boyd, and Yinyu Ye. CVX: Matlab software for disciplined convex programming, 2008.

[18] Toh, K.C., Todd, M.J. and Tutuncu, R.H., SDPT3 – a Matlab Software Package for Semidefinite Programming. *Optimization Methods and Software*, 1999.